

Cite this: DOI: 10.1039/c3bm60139k

## Spontaneous cardiomyocyte differentiation of mouse embryoid bodies regulated by hydrogel crosslink density

Cindy Chung,<sup>a,b</sup> Beth L. Pruitt<sup>b</sup> and Sarah C. Heilshorn<sup>\*a</sup>

Cellular therapies have great potential to provide alternative treatment options for those suffering from heart disease. In order to optimize cell delivery for therapeutic efficacy, a greater understanding of parameters that impact stem cell differentiation, survival, growth, and development are needed. In this study, we examine the role of hydrogel crosslink density on spontaneous cardiomyocyte (CM) differentiation of murine embryoid bodies (EBs). CM differentiation was accelerated in hydrogels of low crosslink density, where 100% of the hydrogels were positive for CM differentiation compared to only 53% in the high crosslink density group after 8 days of culture. DNA microarray data suggests that enhanced CM differentiation in the low crosslink density hydrogels was not tissue specific but rather a result of favoured EB development and cell proliferation. Additionally, enhanced EB growth and differentiation in low crosslink density hydrogels was independent of RGD ligand density and not a consequence of enhanced diffusion. We also demonstrate that matrix metalloproteinase activity is required for spontaneous CM differentiation in 3D hydrogels. Low hydrogel crosslink density regulates spontaneous EB differentiation by promoting EB growth and development. Elucidating the effects of microenvironmental cues on cell differentiation can aid in the optimization of stem cell-based therapies for tissue regeneration.

Received 29th May 2013,  
Accepted 3rd July 2013

DOI: 10.1039/c3bm60139k

[www.rsc.org/biomaterialsscience](http://www.rsc.org/biomaterialsscience)

### Introduction

With heart disease being the number one cause of mortality in the US,<sup>1</sup> the need for cardiac repair and regeneration remedies continues to grow. Since the mid-to-late 1980s, tissue engineering has garnered much attention, emerging as a modern scientific discipline dedicated to the generation of new tissues by utilizing engineering principles in combination with an understanding of biological sciences.<sup>2</sup> In spite of scientific advancements in this field, cellular challenges have hindered translation into clinical application. The production of cells on the scale needed for creating new tissues and ensuring their survival and function within the transplantation site have been major hurdles for the field.<sup>3–6</sup>

With the ability for indefinite self-renewal and differentiation into multiple cell lineages, embryonic stem cells (ESCs) have the potential to be used as a viable cell source for clinical applications. However, in order for ESCs to be useful for medical therapies, a greater understanding of factors that impact their differentiation is essential. Increasing evidence points to the importance of the extracellular matrix (ECM) in

mediating stem cell behavior and fate decisions.<sup>7,8</sup> *In vivo*, the ECM provides a complex network of physical, chemical, and mechanical cues. However, with the development of tunable engineered matrices, we are now able to systematically investigate cellular response to specific matrix properties.

In particular, matrix crosslink density has been shown to play a major role in regulation of cell morphology, growth, and function.<sup>9–13</sup> Highly crosslinked poly(ethylene glycol) hydrogels physically inhibit cell growth in the absence of proteolytic sites.<sup>14</sup> In addition, increased crosslink density has also been shown to inhibit endogenous ECM production and distribution by mesenchymal stem cells undergoing chondrogenic differentiation.<sup>15</sup>

Changes in hydrogel crosslink density can often alter several other hydrogel properties, *e.g.*, modulus, diffusivity, and mesh size. Assuming a homogenous and amorphous hydrogel structure, increases in hydrogel crosslink density would result in increased modulus, decreased diffusivity, and decreased mesh size. Increasing hydrogel crosslink density may also limit the accessibility of the incorporated cell-adhesive ligands, *e.g.*, RGD peptide. RGD peptide is often incorporated into hydrogel networks to promote integrin-mediated adhesion of cells to their surrounding extracellular matrix and subsequent signal transduction from the matrix to cells.<sup>16–18</sup> All of these factors must be considered when analyzing cell response to changes in hydrogel crosslink density.

<sup>a</sup>Materials Science and Engineering, McCullough Building, 476 Lomita Mall, Stanford, CA, USA. E-mail: [heilshorn@stanford.edu](mailto:heilshorn@stanford.edu); Fax: +650 498 5596; Tel: +650 723 3763

<sup>b</sup>Mechanical Engineering, Durand Building, 496 Lomita Mall, Stanford, CA, USA

Previously, we used recombinant elastin-like protein (ELP) hydrogels<sup>19,20</sup> to demonstrate that matrix crosslink density can be used to transiently inhibit the spontaneous contraction of pre-differentiated embryoid bodies (EBs) encapsulated in 3D matrices. When contracting EBs were encapsulated in ELP hydrogels of high crosslink density, contractile behaviour was transiently suspended. However, embryonic stem cell-derived cardiomyocytes were capable of adapting to the higher cross-linked network with recovered contractility after a period of culture time, suggesting an adaptation of the cells to their surrounding ECM. Here, we examine the role of matrix crosslink density and RGD-mediated integrin adhesion on CM differentiation with interest in how crosslink density affects cell gene expression, growth, and matrix remodeling with a 3D hydrogel environment.

## Materials and methods

### Elastin-like protein (ELP) expression and purification

As previously reported,<sup>20</sup> ELP (Fig. 1A) was expressed and purified using standard recombinant protein technology. Briefly, genes encoding the desired protein sequences were cloned into pET15b plasmids using traditional recombinant techniques, expressed in *Escherichia coli*, BL21(DE3), for 3–5 h, and purified using an inverse temperature-cycling process. Typical protein yields were 50–100 mg l<sup>-1</sup>. The modular protein design consisted of four repeats of a bioactive domain and a structural elastin-like domain ((VPGIG)<sub>2</sub>VPGKG(VPGIG)<sub>2</sub>)<sub>3</sub>. The bioactive domain consisted of an extended RGD sequence derived from fibronectin (TVYAVTGRGDSPASSAA). An ELP variant with a scrambled RDG sequence (labeled as 0 mM RGD) was used for comparison in experiments isolating RGD cell-adhesion effects.

### Hydrogel formation and characterization

Recombinant protein chains were crosslinked through lysine residues using tetrakis hydroxymethyl phosphonium chloride (THPC, Sigma),<sup>21</sup> where hydrogel crosslink density was tuned

by varying THPC to protein primary amine reactive group stoichiometry (0.5:1, 0.75:1, and 1:1). Acellular 5 wt% ELP hydrogels were tested in unconfined compression on an ARG2 rheometer (TA Instruments). Briefly, ELP hydrogels (50 μl) were crosslinked in cylindrical molds (8 mm diameter) for 10 min at room temperature followed by 10 min at 37 °C. Molds were removed, and hydrogels were compressed at 2 μm s<sup>-1</sup> at 37 °C in a custom-made phosphate buffered saline (PBS) bath. Elastic modulus in compression was determined by taking the slope of the stress-strain curve for small strains (<15%). Effective diffusion coefficients were determined from fluorescent recovery after photobleaching (FRAP) experiments. Fluorescein isothiocyanate (FITC)-labeled dextran (70 kDa, Sigma) was encapsulated at 4 mg ml<sup>-1</sup> in 5 wt% ELP hydrogels of different crosslink densities in custom molds (3 mm in diameter and 0.5 mm in height). FRAP experiments were performed on a Leica SPE confocal microscope. A 100 micron by 100 micron region of the image was photobleached with a 488 nm laser at 100% intensity for 15 seconds. A time series was captured every 1.6 seconds for 2 minutes to capture fluorescent recovery. The time series was analyzed using open source matlab code “frap\_analysis” to determine the effective diffusion coefficient within the hydrogels.<sup>22</sup> Values are reported as mean ± SEM.

### Murine embryonic stem cell culture and cardiomyocyte differentiation

Mouse ESCs (CGR8) that express EGFP under transcriptional control of a cardiac-specific promoter ( $\alpha$ -myosin heavy chain)<sup>23</sup> were used to monitor CM differentiation. ESCs were cultured on 0.25% gelatin-coated tissue culture polystyrene in Glasgow minimum essential medium supplemented with knockout serum replacement and 1000 U ml<sup>-1</sup> leukemia inhibitory factor (LIF). Differentiation was induced by embryoid body formation via the hanging drop technique in medium supplemented with 15% fetal bovine serum and the removal of LIF. After 2 days, EBs were removed from hanging drops and immediately encapsulated in 5 wt% ELP hydrogels with 1–3 embryoid bodies per 2.5 μl gel. Samples were cultured in differentiation

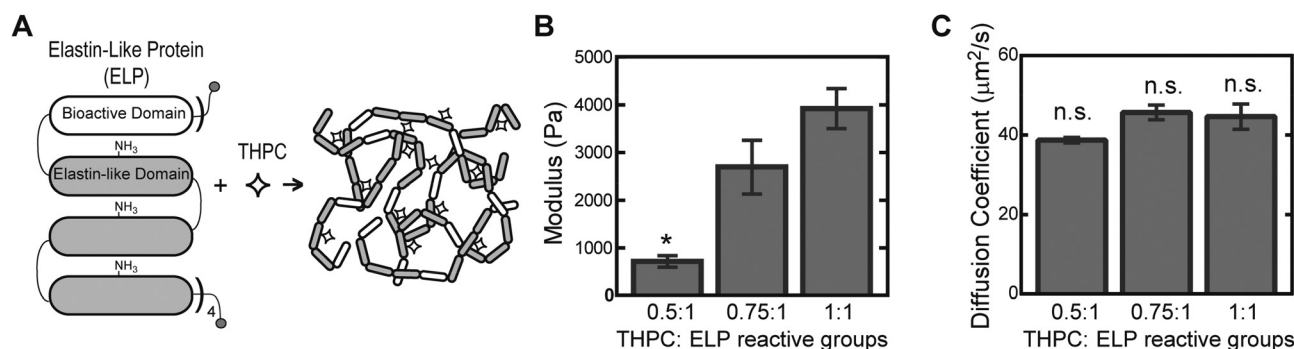


**Fig. 1** Schematic of ELP hydrogel formation. ELP consists of 4 repeats of a cassette containing 1 bioactive domain and 3 identical elastin-like domains, which include lysine residues within the elastin-like domain to provide amine reactive crosslinking sites that form covalent bonds with THPC (A). Elastic moduli of 5 wt% ELP hydrogels ( $n = 4$ – $5$ ) with varying THPC: ELP reactive group stoichiometry (B). Effective diffusion coefficient for 70 kDa FITC-dextran in 5 wt% ELP hydrogels of varying crosslink density (C). All values are reported as mean ± SEM, where \* denotes significant difference and n.s. denotes no significant difference,  $p < 0.05$ .

medium supplemented with 100 mg ml<sup>-1</sup> L-ascorbic acid, with media changes every other day. EGFP expression and cell contractility was monitored visually on a Leica SPE confocal microscope every other day post encapsulation. The percentage of total hydrogels expressing EGFP, the percentage of hydrogels contracting, and the contractility rate were recorded. Significant differences in EGFP expression and contractility among groups were determined using  $\chi^2$  tests for binomial distributions with  $\alpha = 0.05$ . Experiments were repeated 3 times, where one representative data set was chosen due to slight shifts in differentiation timeline as a result of the different batches of cells used.

#### RNA extraction and DNA microarray analysis

DNA microarray analysis was performed after 8 days of culture. Four hydrogels (1 EB per 2.5  $\mu$ l gel) were pooled into one sample and homogenized in Trizol Reagent (Invitrogen) with Qiagen TissueRuptor. RNA was extracted according to manufacturer's instructions. RNA concentration was determined using a Nanodrop spectrophotometer, and RNA quality was verified using the Agilent 2100 Bioanalyzer. Samples ( $n = 4$ ) were run on a mouse Ref-8 beadchip (Illumina) at the Stanford Functional Genomics Facility. Gene expression analysis was performed using Partek Genomic Suite. An ANOVA comparing hydrogels at 0.5 : 1 and 1 : 1 crosslink densities in 5 wt% ELP hydrogels with 5.3 mM RGD ligands was performed. Using a false discovery rate (FDR) <0.05, a gene list of differentially regulated genes was created and examined using Ingenuity Pathway Analysis to determine the top up-regulated and down-regulated biological functions.

#### Metabolic activity and cellular outgrowth

Metabolic activity of encapsulated EBs was assessed using PrestoBlue® cell viability reagent (Invitrogen) after 1, 4, and 8 days of culture. PrestoBlue® reagent, diluted 10-fold in differentiation medium, was added to samples ( $n = 3$ ) and incubated for 3 h. Fluorescence readings were measured using an excitation of 560 nm and an emission of 590 nm. Cell proliferation was quantified using PicoGreen dsDNA assay after 1, 4, and 8 days of culture. Additionally, cellular outgrowth was visualized and characterized by the extent of cell coverage within the hydrogel after 8 days of culture. Samples were fixed in 4% paraformaldehyde and stained with 4',6-diamidino-2-phenylindole (DAPI, Invitrogen) for nuclear visualization. Images were obtained on a Leica SPE confocal microscope. Using maximum projections of each z-stack, pixel intensity quantification was used to quantify the percentage of cell coverage.

#### Matrix metalloproteinase (MMP) activity and inhibition

To monitor cell-dictated matrix remodeling, active MMPs within the hydrogels were assayed after 8 days of culture using a Sensolyte 520 MMP assay (Anaspec) according to manufacturer's instructions. After removing cell culture media, 3 hydrogels (1 EB per 2.5  $\mu$ l gel) were pooled into one sample and homogenized in lysis buffer. MMP activity was normalized to DNA content as determined using PicoGreen dsDNA assay ( $n =$

3 samples). To determine if CM differentiation was correlated to the ability of cells to initiate matrix remodeling, embryoid bodies encapsulated in ELP hydrogels of the lowest crosslink density were treated with the addition of soluble, broad spectrum MMP inhibitor (PD166793, 100  $\mu$ M, Sigma) or doxycycline (100  $\mu$ M, Sigma) ( $n = 11$ –14). CM differentiation was assessed by monitoring EGFP expression as described above.

## Results

Engineered matrices serve as useful tools in the exploration of cellular response to microenvironmental parameters. For example, we have previously used ELP hydrogels to tailor neurite growth from dorsal root ganglia<sup>24</sup> and to transiently inhibit embryonic stem cell-derived cardiomyocyte contractility<sup>19</sup> by varying matrix properties like cell adhesivity and crosslink density. In this study, we utilized recombinantly engineered ELPs to investigate matrix effects on the spontaneous CM differentiation of murine EBs in three dimensional hydrogels.

#### ELP hydrogel characterization

Changes in crosslink density, tuned by varying crosslinker to protein stoichiometry, was reflected in mechanical properties, with elastic moduli ranging from 715  $\pm$  120 to 3919  $\pm$  420 Pa for 0.5 : 1 and 1 : 1 crosslinking groups, respectively (Fig. 1B). As expected, elastic moduli increases as THPC to ELP reactive group ratio approaches 1 : 1. To address the potential effects of limitations in nutrient and waste diffusion within hydrogels of different crosslink densities, FRAP experiments were conducted. For all hydrogels, similar effective diffusion coefficients for 70 kDa FITC-labeled dextran was observed, demonstrating that observed cellular effects among hydrogels of different crosslink densities would not be a consequence of diffusional limitations (Fig. 1C).

#### Spontaneous cardiomyocyte differentiation

Murine ESCs spontaneously differentiate when cultured in three dimensional hydrogels. When cultured in hydrogels of different crosslink densities, they differentiate at varying rates (Fig. 2). Using a EGFP reporter under a cardiac-specific promoter, CM differentiation was monitored optically for 8 days of culture. Murine EBs in hydrogels with the lowest crosslink density, *i.e.* 0.5 : 1 THPC to ELP reactive group stoichiometry, exhibited accelerated EGFP expression when compared to higher crosslink density groups. Significant differences in EGFP expression were observed at days 4, 6, and 8 (Fig. 2B). By day 8, 100% of the 0.5 : 1 hydrogels were positive for EGFP expression compared to only 53% in the 1 : 1 group.

Contractility rate was used as an assessment of CM function. Despite the delayed CM differentiation in the higher crosslinking groups, no significant differences were observed in beat rate among all groups when corrected for the first day of spontaneous contraction (Fig. 3B). Even though no differences were observed among the groups, a general increase in

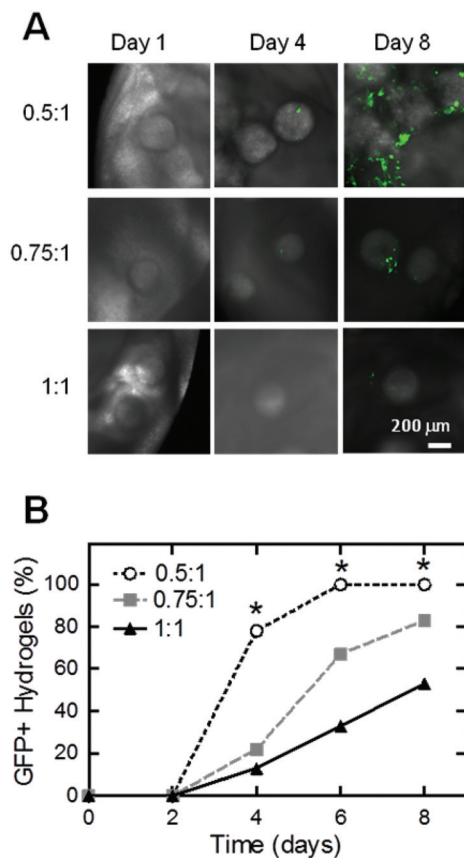


**Fig. 2** Representative fluorescent images of EGFP expression within hydrogels after 2, 4, and 8 days of culture for crosslink densities of 0.5 : 1, 0.75 : 1, and 1 : 1 THPC to ELP reactive groups (A). Yield of EGFP positive hydrogels ( $n = 15-18$ ), where \* denotes significant difference among groups ( $p < 0.05$ ) by  $\chi^2$  test for binomial distributions (B).

beat rate was observed with time for all conditions. To delve into the underlying causes for the differences in CM differentiation rate, we looked at murine EB gene expression through DNA microarrays, murine EB outgrowth, and the ability of the cells to remodel their surrounding matrix.

### EB gene expression

DNA microarray analysis indicated significant differences in gene expression levels between murine EBs encapsulated in ELP hydrogels of 0.5 : 1 and 1 : 1 crosslink densities. Genes exhibiting significantly different gene regulation ( $p < 0.05$ ) were analyzed for functional pathway enrichment. In comparing the 0.5 : 1 to 1 : 1 crosslink densities, genes associated with organism, embryonic, and tissue development, along with cellular assembly and organization were significantly up-regulated, while genetic programs related to cell death and disease were significantly down-regulated (Fig. 4). No significant differences were observed between 0.5 : 1 and 1 : 1 hydrogels crosslink density groups when looking for specific cardiac markers: GATA-4 ( $p = 0.4$ ),  $\alpha$ -myosin heavy chain ( $p = 0.15$ ), cardiac troponin I ( $p = 0.93$ ), connexin 43 ( $p = 0.42$ ). Though differential expression for transcription factor NKX2-5 ( $p = 0.04$ ) was

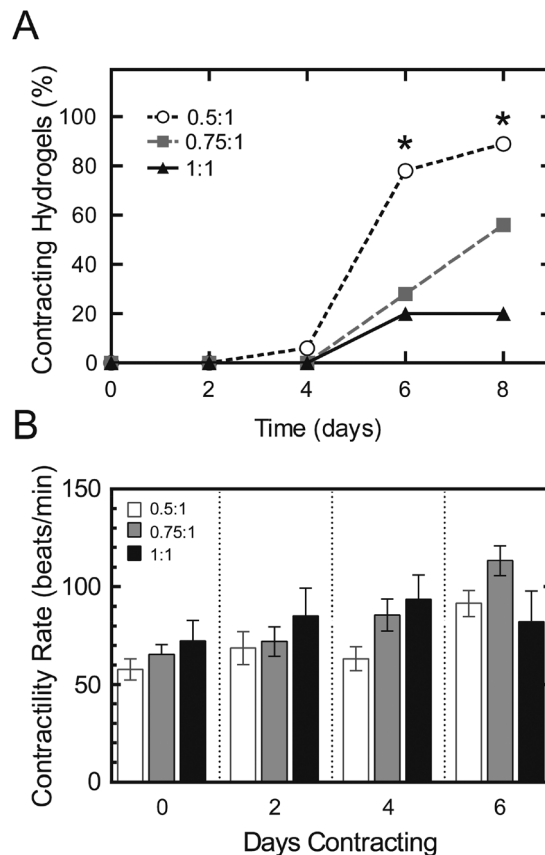


**Fig. 3** Yield of contracting hydrogels (A) and contractility rate (B) plotted for each hydrogel-encapsulated embryoid body exhibiting contractile behavior for up to 8 days. Data are displayed as the mean and SEM for each group ( $n = 8-14$ ). Significant differences among groups ( $p < 0.05$ ) using  $\chi^2$  test for binomial distributions is denoted by \*. No significant differences in contractility rates were observed among all groups.

observed, relative gene expression was not substantially up-regulated (0.5 : 1/1 : 1 = 1.08), where a 0.5 : 1/1 : 1 = 1 would represent no fold change.

### EB survival, proliferation and outgrowth

To look at cellular response to crosslink density effects downstream of gene expression, EB viability, proliferation, and outgrowth were also quantified. EBs demonstrated an increase in both metabolic activity and proliferation of cells (as quantified by DNA content) in the 0.5 : 1 group compared to the 1 : 1 crosslink density hydrogels with significant differences noted at later time points (Fig. 5A and B). Further support for increased murine EB outgrowth in hydrogels of lower crosslink density was observed when cell nuclei were stained with DAPI to visualize cell coverage within the hydrogels, where greater cell coverage was found for the 0.5 : 1 group compared to the 1 : 1 group (Fig. 5C).

By using a negative control ELP containing a non-adhesive, scrambled RDG sequence for comparison, control experiments were performed to isolate the effects of the RGD ligand. Interestingly, these studies clearly demonstrate that murine EB survival, proliferation, and growth were independent of RGD ligand presence (Fig. 5). No significant differences were found

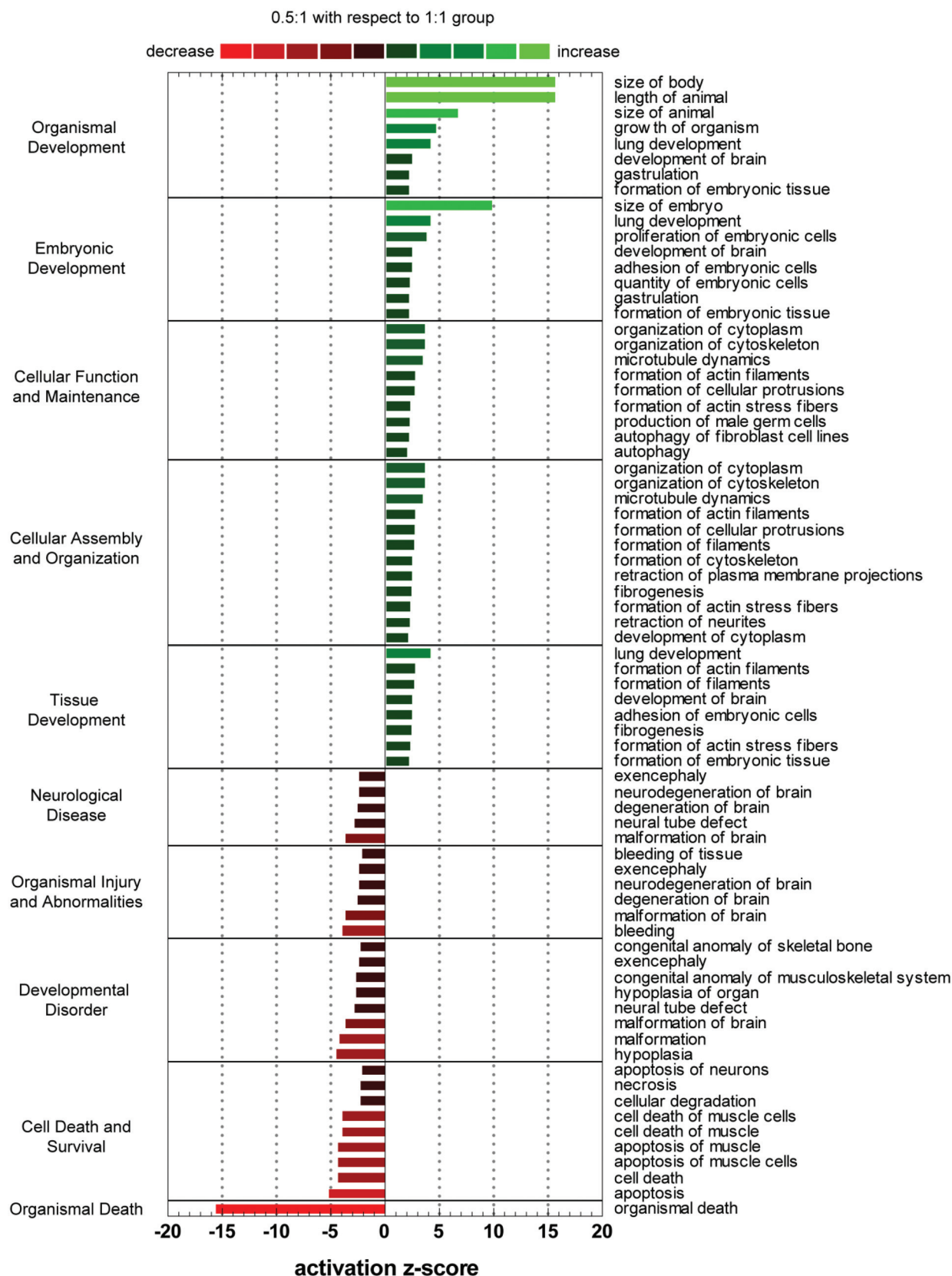


**Fig. 4** Functional pathway enrichment analysis of genes differentially regulated ( $p < 0.05$ ) between 0.5 : 1 and 1 : 1 crosslink density groups. Top five up and down regulated categories are presented, where the magnitude of functional increase (green) or decrease (red) of 0.5 : 1 group over 1 : 1 group for respective processes are indicated by activation z-score.

among ELP hydrogels with the same crosslink density that contained the RGD adhesive sequence or the inactive RDG sequence.

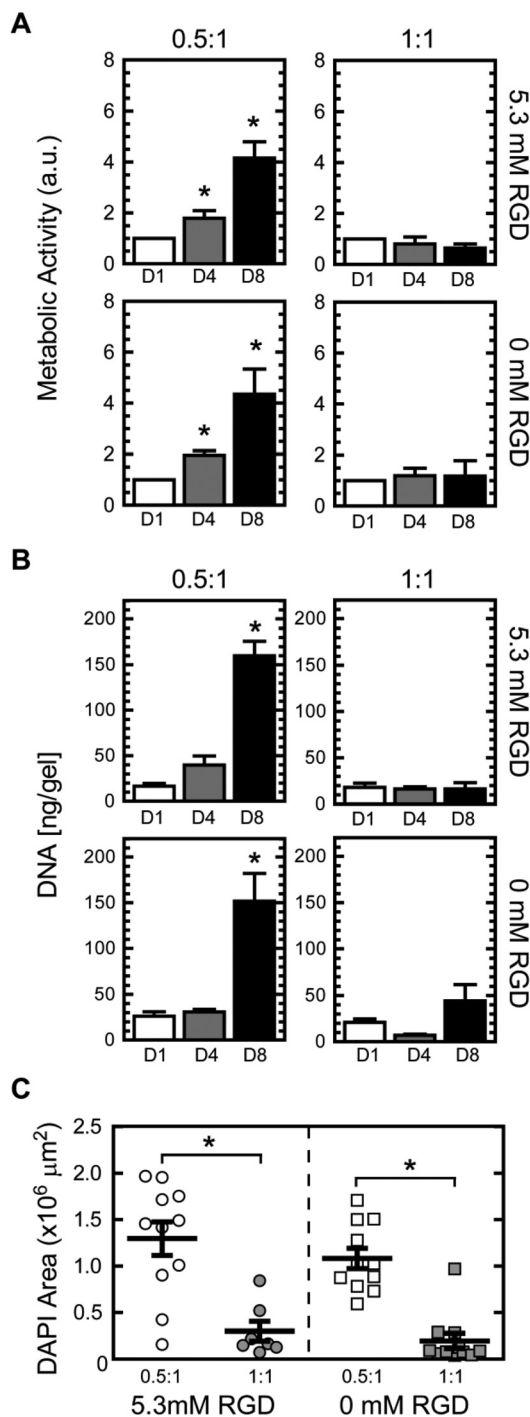


**Fig. 5** Metabolic activity ( $n = 5-6$ ) (A) and DNA content ( $n = 11-12$ ) (B) for murine EBs encapsulated in 5 wt% ELP hydrogels of 0.5:1 and 1:1 crosslink density, with 5.3 or 0 mM RGD ligand density, at days 1, 4, and 8. DAPI coverage ( $n = 7-11$ ) of murine EBs encapsulated after 8 days of culture (C). Significant difference ( $p < 0.05$ ) compared to 1:1 counterparts determined by Tukey's posthoc test is denoted by \*. No significant differences were observed between 0 (using scrambled RDG ELP variant) and 5.3 mM RGD hydrogels at the same crosslink density.

### Cell-dictated matrix remodeling

To monitor cell-dictated matrix remodeling, MMP activity was quantified within the hydrogels. Similar to the murine EB outgrowth results, RGD ligand presence had little effect on MMP activity of the cells compared to the effects of crosslink density (Fig. 6), where greater MMP activity per DNA content was observed in the lower crosslinking group. By normalizing to DNA content, MMP activity is normalized for cell proliferation, indicating that in addition to promoting cellular growth, the 0.5:1 crosslink density group also favors greater MMP activity per cell.

To investigate the role of MMPs in spontaneous CM differentiation, MMP inhibitors were added to the culture media of 0.5:1 hydrogels. Compared to the control group without the addition of MMP inhibitors, the addition of soluble MMP inhibitors (PD166793 and doxycycline) impeded cell outgrowth and resulted in delayed CM differentiation (Fig. 7). Interestingly, this delay was not as pronounced as that observed when crosslink density of the hydrogel is increased (Fig. 2B). MMP-inhibited 0.5:1 hydrogels continued to permit CM differentiation with greater yields than that of hydrogels with higher crosslink densities.

### Discussion

Adult cardiomyocytes have limited proliferative capacity,<sup>25</sup> so loss of cardiomyocytes due to myocardial infarction and disease can lead to irreparable loss of heart function. With current therapies only delaying heart disease progression or requiring organ transplantation, a great clinical need exists for the production of cardiomyocytes. Researchers have turned towards pluripotent stem cells, using engineered systems to study CM differentiation,<sup>10,26-28</sup> to address this need. Embryonic stem cells have been clustered into EBs and cultured in suspension,<sup>29,30</sup> in microwells,<sup>31,32</sup> and in hydrogels of varying natural<sup>33</sup> and synthetic<sup>10,34</sup> materials to study the differentiation process. Though it is difficult to compare across the different culture systems, each controlled study sheds light on

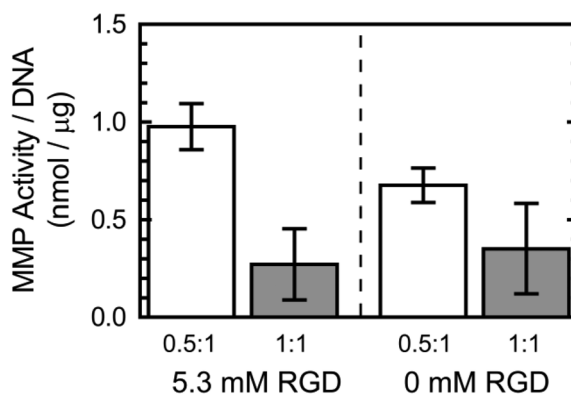


**Fig. 6** MMP activity within 5 wt% ELP hydrogels with 5.3 or 0 mM RGD ligand density at 0.5:1 and 1:1 crosslink density ( $n = 3$ ).

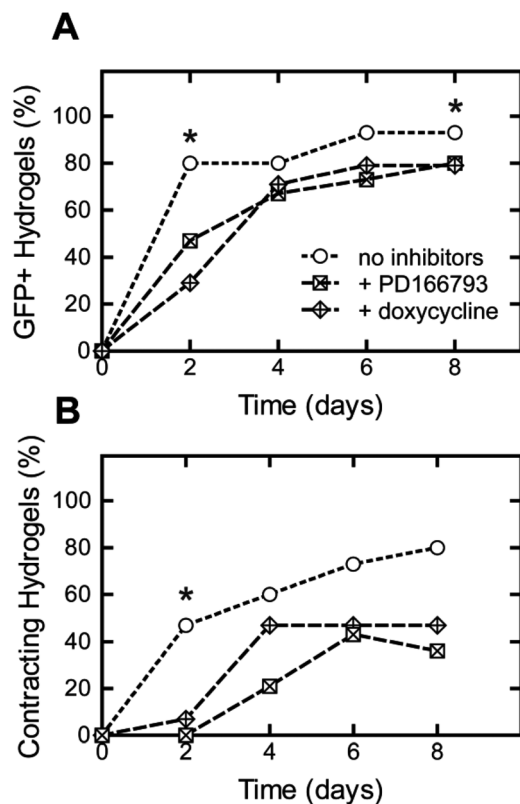


**Fig. 7** Cardiomyocyte differentiation yield within 5 wt% ELP hydrogels with 0.5 : 1 crosslink density and 5.3 mM RGD ligand density quantified by EGFP expression (A) and contractility (B) with or without the addition of MMP inhibitors, PD166793 and doxycycline ( $n = 11-14$ ). Significant differences among groups ( $p < 0.05$ ) using  $\chi^2$  test for binomial distributions is denoted by \*.

the effects of various parameters, *e.g.*, embryoid body size, cell adhesion, chemical cues, and physical cues, on directed differentiation of ESCs.

Engineered matrices have been developed as tools to investigate extracellular matrix (ECM) effects on cell behavior. Using modular designs, matrix parameters can be independently tuned to isolate specific matrix effects in hopes of deconstructing complex micro-environmental cues. In particular, recombinant ELPs, attractive for their ability to mimic the modulus of native cardiac tissue and their resilience to withstand repeated strains during cell contraction, can be crosslinked into hydrogels of varying crosslink density while maintaining constant RGD cell-adhesive ligand density and protein weight percent.<sup>20</sup> Previously, we have shown that ELP hydrogel crosslink density could modulate transient contractile inhibition of human embryoid bodies that had been allowed to spontaneously differentiate into cardiomyocytes prior to encapsulation.<sup>19</sup> In this study, we investigated the spontaneous CM differentiation of mouse EBs within hydrogels of varying crosslink density, focusing on how crosslink density affects gene expression, cell growth, and matrix remodeling.

CM differentiation was temporally accelerated in hydrogels with lower crosslink density (0.5 : 1) (Fig. 2). DNA microarray data indicated significant differences in gene expression levels

between murine EBs encapsulated in ELP hydrogels of 0.5 : 1 and 1 : 1 crosslink densities. Surprisingly, differentially regulated genes were not cell-lineage specific, but rather more indiscriminate, demonstrating that hydrogels of 0.5 : 1 crosslink density provided a more supportive environment for overall EB development (Fig. 4). Genes associated with growth, assembly, and organization (from the cell to organism scale) were significantly up-regulated, while death and disease were significantly down-regulated. Thus, the observed increases in CM differentiation in hydrogels with lower crosslink densities (0.5 : 1), could be a reflection of general EB growth and development.

Despite good viability of mouse EBs in all groups as previously reported,<sup>21</sup> large differences were observed in how the cells grew and spread (Fig. 5) within hydrogels of low and high crosslink density. While hydrogels with high crosslink densities of other materials have been reported to experience diffusional limitations, we found that the diffusion of 70 kDa dextran was not restricted within the 1 : 1 hydrogels (Fig. 1C). As most paracrine signals secreted by cells are smaller than 70 kDa, these signals are likely smaller than the hydrogel mesh size and are capable of diffusing within hydrogels of low and high crosslink densities at similar rates. Thus, the effects of diffusional limitations in cell signaling and nutrient and waste transport are expected to be negligible in dictating cellular response.

Increasing hydrogel crosslink density may also limit the accessibility of the incorporated RGD ligands. To address this concern, ELPs including a scrambled, non-cell adhesive RDG domain were used for comparison. In some poly (ethylene glycol) systems, the addition of RGD ligands reduced EB aggregation and promoted endothelial differentiation; however, crosslink density was not specifically controlled.<sup>34</sup> Our results (Fig. 5) show that the presence of RGD ligand was not essential for mouse EB metabolic activity, growth, and proliferation in the ELP hydrogels, demonstrating that crosslink density was the key parameter in EB growth regulation. Increases in crosslink density, or decreases in mesh size, have been shown to inhibit cell growth in other cell-laden 3D hydrogel systems.<sup>14,35</sup> Accordingly, hydrogels of lower crosslink density contain greater voids and spaces, permitting cells to grow, spread, and subsequently differentiate. Crosslink density can also affect the local deposition of EB secreted proteins, which may drive EB differentiation patterns.<sup>36</sup> It is important to note the differences among hydrogel culture systems. In this study, we focused on the differentiation of individual EBs, and we were able to control crosslink density while varying RGD ligand density independently to determine cell adhesive ligand effects.

To determine if the delayed CM differentiation was the result of the restricted ability for cells to remodel the surrounding matrix, mouse EB-laden hydrogels were assayed for MMP activity. MMPs represent the main group of regulating proteases in the ECM. MMPs induce ECM remodeling, which is essential for cell migration, proliferation, and differentiation during normal development.<sup>37,38</sup> Hydrogels of lower crosslink

density exhibited greater MMP activity per DNA content (Fig. 6). Increased crosslink density can result in restricted matrix distribution within hydrogels.<sup>15</sup> Chen *et al.* has shown that ESCs are dependent on endogenous ECM for survival and differentiation.<sup>39</sup> Thus, higher crosslink density in the 1:1 hydrogels could limit endogenous matrix deposition, and subsequently lower MMP remodeling activity. Additionally, during CM differentiation, cardiomyocyte progenitor cells (CPCs) have shown increased expression of genes associated with extracellular matrix synthesis (*e.g.* collagen type I, III, and IV, fibronectin, and elastin) and matrix remodeling (*e.g.* MMP -2 and -9, and tissue inhibitor of metalloproteinase (TIMP) -1, -2, and -4) compared to non-differentiating CPCs.<sup>40</sup> Thus, the observed increase in MMP activity within the 0.5:1 hydrogels may be correlated to CM differentiation.

To investigate the role of matrix remodeling, encapsulated mouse EBs in 0.5:1 hydrogels were treated with exogenous, broad-spectrum MMP inhibitors, PD166793 and doxycycline. The addition of soluble MMP inhibitors delayed and decreased the yield of CM differentiation (Fig. 7). This effect was most notable early in the culture. As the cells continued to grow and proliferate in the 0.5:1 hydrogels with culture time, EB development could trigger increased matrix remodeling activity that may overcome the effects of the MMP inhibitors. Overall, the delayed differentiation suggests that cell-dictated matrix remodeling does play a role in spontaneous cardiac differentiation. This matrix remodeling is likely local to the EBs, as no visible bulk gel degradation was observed after two weeks of culture in previous studies with ELP hydrogels.<sup>19</sup>

With changes in crosslink density, ELP hydrogel modulus is also altered (Fig. 1B). Studies in 2D have shown that substrate modulus can influence pluripotency and differentiation of embryonic stem cells.<sup>41,42</sup> Substrates with elasticity matching native tissue of the desired cell type are thought to favor cell fate decisions towards the desired cell-lineage and cell maturation.<sup>43-45</sup>

In a 3D matrix metalloproteinase-sensitive poly (ethylene glycol) hydrogel system, compliant hydrogels ~300 Pa, mimicking the elasticity of embryonic cardiac tissue, demonstrated increased expression of cardiac transcription factor, NKX2-5, while stiffer hydrogels ~4000 Pa showed decreased expression.<sup>10</sup> Here we demonstrate similar results, where our compliant hydrogel promoted cardiomyocyte differentiation. Given the compliant nature of the ELP hydrogel system, we would expect greater differentiation towards neural, cardiac, and muscle lineages as opposed to cartilage or bone.

## Conclusions

In this study, we investigated the spontaneous CM differentiation of mouse EBs in ELP hydrogels of varying crosslink density, focusing on how crosslink density affects cell gene expression, growth, and matrix remodeling. With the careful design of engineered matrices, we isolated the effects of crosslink density on CM differentiation without altering protein

and RGD ligand concentration. Here, we have shown that hydrogels with lower crosslink density accelerate CM differentiation in 3D hydrogels by permitting cellular growth, proliferation, and cell-dictated ECM remodeling. This effect was independent of RGD ligand and diffusional limitations of nutrients and waste. Elucidating the effects of microenvironmental cues on cell differentiation can aid in the optimization of stem cell-based therapies for tissue regeneration.

## Acknowledgements

The authors thank R.T. Lee and R.D. Kamm for the generous gift of mouse ESCs that express EGFP under transcriptional control of a cardiac-specific promoter ( $\alpha$ -myosin heavy chain), Karen Dubbin for help with FRAP experiments, and Rebecca Taylor for helpful discussions. Additionally, the authors thank the Stanford Functional Genomics Facility and Vida Shokoohi for help in generating DNA microarray data. The authors acknowledge funding support from NIH 1DP2OD006477 (SCH), NIH 1R01 DK0085720 (SCH), NIH 1R21AR06235901 (SCH), NSF DMR-0846363 (SCH), NSF EFRI-CBE 0735551 (BLP) and AHA 10POST4190103 (CC).

## Notes and references

- 1 D. Lloyd-Jones, R. J. Adams, T. M. Brown, M. Carnethon, S. Dai, G. De Simone, T. B. Ferguson, E. Ford, K. Furie, C. Gillespie, A. Go, K. Greenlund, N. Haase, S. Hailpern, P. M. Ho, V. Howard, B. Kissela, S. Kittner, D. Lackland, L. Lisabeth, A. Marelli, M. M. McDermott, J. Meigs, D. Mozaffarian, M. Mussolino, G. Nichol, V. L. Roger, W. Rosamond, R. Sacco, P. Sorlie, T. Thom, S. Wasserthiel-Smoller, N. D. Wong and J. Wylie-Rosett, *Circulation*, 2009, **121**, e46–e215.
- 2 R. Langer and J. P. Vacanti, *Science*, 1993, **260**, 920–926.
- 3 H. J. Kong, M. K. Smith and D. J. Mooney, *Biomaterials*, 2003, **24**, 4023–4029.
- 4 M. A. Laflamme, K. Y. Chen, A. V. Naumova, V. Muskheli, J. A. Fugate, S. K. Dupras, H. Reinecke, C. Xu, M. Hassanipour, S. Police, C. O'Sullivan, L. Collins, Y. Chen, E. Minami, E. A. Gill, S. Ueno, C. Yuan, J. Gold and C. E. Murry, *Nat. Biotechnol.*, 2007, **25**, 1015–1024.
- 5 S. B. Seif-Naraghi, M. A. Salvatore, P. J. Schup-Magoffin, D. P. Hu and K. L. Christman, *Tissue Eng. A*, 2010, **16**, 2017–2027.
- 6 G. Zhang, Q. Hu, E. A. Braunlin, L. J. Suggs and J. Zhang, *Tissue Eng. A*, 2008, **14**, 1025–1036.
- 7 C. J. Flaim, S. Chien and S. N. Bhatia, *Nat. Methods*, 2005, **2**, 119–125.
- 8 F. Yang, S. W. Cho, S. M. Son, S. P. Hudson, S. Bogatyrev, L. Keung, D. S. Kohane, R. Langer and D. G. Anderson, *Bio-macromolecules*, 2010, **11**, 1909–1914.
- 9 S. J. Bryant, K. S. Anseth, D. A. Lee and D. L. Bader, *J. Orthop. Res.*, 2004, **22**, 1143–1149.



- 10 T. P. Kraehenbuehl, P. Zammaretti, A. J. Van der Vlies, R. G. Schoenmakers, M. P. Lutolf, M. E. Jaconi and J. A. Hubbell, *Biomaterials*, 2008, **29**, 2757–2766.
- 11 K. A. Kyburz and K. S. Anseth, *Acta Biomater.*, 2013, **9**, 6381–6392.
- 12 A. Marsano, R. Maidhof, L. Q. Wan, Y. Wang, J. Gao, N. Tandon and G. Vunjak-Novakovic, *Biotechnol. Prog.*, 2010, **26**, 1382–1390.
- 13 K. Shapira-Schweitzer and D. Seliktar, *Acta Biomater.*, 2007, **3**, 33–41.
- 14 K. Bott, Z. Upton, K. Schrobback, M. Ehrbar, J. A. Hubbell, M. P. Lutolf and S. C. Rizzi, *Biomaterials*, 2010, **31**, 8454–8464.
- 15 L. Bian, C. Hou, E. Tous, R. Rai, R. L. Mauck and J. A. Burdick, *Biomaterials*, 2013, **34**, 413–421.
- 16 D. Choquet, D. P. Felsenfeld and M. P. Sheetz, *Cell*, 1997, **88**, 39–48.
- 17 D. L. Hern and J. A. Hubbell, *J. Biomed. Mater. Res.*, 1998, **39**, 266–276.
- 18 M. D. Pierschbacher and E. Ruoslahti, *Nature*, 1984, **309**, 30–33.
- 19 C. Chung, E. Anderson, R. R. Pera, B. L. Pruitt and S. C. Heilshorn, *Soft Matter*, 2012, **8**, 10141–10148.
- 20 K. S. Straley and S. C. Heilshorn, *Soft Matter*, 2009, **5**, 114–124.
- 21 C. Chung, K. J. Lampe and S. C. Heilshorn, *Biomacromolecules*, 2012, **13**, 3912–3916.
- 22 P. Jonsson, M. P. Jonsson, J. O. Tegenfeldt and F. Hook, *Biophys. J.*, 2008, **95**, 5334–5348.
- 23 T. Takahashi, B. Lord, P. C. Schulze, R. M. Fryer, S. S. Sarang, S. R. Gullans and R. T. Lee, *Circulation*, 2003, **107**, 1912–1916.
- 24 K. J. Lampe, A. L. Antaris and S. C. Heilshorn, *Acta Biomater.*, 2013, **9**, 5590–5599.
- 25 M. H. Soonpaa and L. J. Field, *Circ. Res.*, 1998, **83**, 15–26.
- 26 Y. Y. Choi, B. G. Chung, D. H. Lee, A. Khademhosseini, J. H. Kim and S. H. Lee, *Biomaterials*, 2010, **31**, 4296–4303.
- 27 Y. Duan, Z. Liu, J. O'Neill, L. Q. Wan, D. O. Freytes and G. Vunjak-Novakovic, *J. Cardiovasc. Transl. Res.*, 2011, **4**, 605–615.
- 28 J. L. Young and A. J. Engler, *Biomaterials*, 2011, **32**, 1002–1009.
- 29 W. He, L. Ye, S. Li, H. Liu, Q. Wang, X. Fu, W. Han and Z. Chen, *Biol. Pharm. Bull.*, 2012, **35**, 308–316.
- 30 C. Y. Sargent, G. Y. Berguig, M. A. Kinney, L. A. Hiatt, R. L. Carpenedo, R. E. Berson and T. C. McDevitt, *Biotechnol. Bioeng.*, 2010, **105**, 611–626.
- 31 Y. S. Hwang, B. G. Chung, D. Ortmann, N. Hattori, H. C. Moeller and A. Khademhosseini, *Proc. Natl. Acad. Sci. U. S. A.*, 2009, **106**, 16978–16983.
- 32 J. C. Mohr, J. Zhang, S. M. Azarin, A. G. Soerens, J. J. de Pablo, J. A. Thomson, G. E. Lyons, S. P. Palecek and T. J. Kamp, *Biomaterials*, 2010, **31**, 1885–1893.
- 33 Y. Duan, Z. Liu, J. O'Neill, L. Q. Wan, D. O. Freytes and G. Vunjak-Novakovic, *J. Cardiovasc. Transl. Res.*, 2011, **4**, 605–615.
- 34 L. Schukur, P. Zorlutuna, J. M. Cha, H. Bae and A. Khademhosseini, *Adv. Healthc. Mater.*, 2013, **2**, 195–205.
- 35 S. Khetan and J. A. Burdick, *Biomaterials*, 2010, **31**, 8228–8234.
- 36 G. G. Giobbe, M. Zagallo, M. Riello, E. Serena, G. Masi, L. Barzon, B. Di Camillo and N. Elvassore, *Biotechnol. Bioeng.*, 2012, **109**, 3119–3132.
- 37 S. Augustin, M. Berard, S. Kellaf, N. Peyri, F. Fauvel-Lafeve, C. Legrand, L. He and M. Crepin, *Anticancer Res.*, 2009, **29**, 1335–1343.
- 38 J. D. Mott and Z. Werb, *Curr. Opin. Cell Biol.*, 2004, **16**, 558–564.
- 39 S. S. Chen, W. Fitzgerald, J. Zimmerberg, H. K. Kleinman and L. Margolis, *Stem Cells*, 2007, **25**, 553–561.
- 40 N. A. Bax, M. H. van Marion, B. Shah, M. J. Goumans, C. V. Bouten and D. W. van der Schaft, *J. Mol. Cell Cardiol.*, 2012, **53**, 497–508.
- 41 F. Chowdhury, Y. Li, Y. C. Poh, T. Yokohama-Tamaki, N. Wang and T. S. Tanaka, *PLoS One*, 2010, **5**, e15655.
- 42 N. D. Evans, C. Minelli, E. Gentleman, V. LaPointe, S. N. Patankar, M. Kallivretaki, X. Chen, C. J. Roberts and M. M. Stevens, *Eur. Cell Mater.*, 2009, **18**, 1–13; discussion 13–14.
- 43 P. Bajaj, X. Tang, T. A. Saif and R. Bashir, *J. Biomed. Mater. Res. A*, 2010, **95**, 1261–1269.
- 44 B. Bhana, R. K. Iyer, W. L. Chen, R. Zhao, K. L. Sider, M. Likhitpanichkul, C. A. Simmons and M. Radisic, *Biotechnol. Bioeng.*, 2010, **105**, 1148–1160.
- 45 J. G. Jacot, A. D. McCulloch and J. H. Omens, *Biophys. J.*, 2008, **95**, 3479–3487.